RESEARCH ARTICLE

WILEY | JCN RESEARCH IN SYSTEMS NEUROSCIENCE THE JOURNAL OF COMPARATIVE NEUROLOGY

Cortical connections of area 2 and posterior parietal area 5 in macaque monkeys

Jeffrey Padberg[1] 🄳 | Dylan F. Cooke[2] | Christina M. Cerkevich[3,4] |
Jon H. Kaas[4] 🄳 | Leah Krubitzer[5,6]

[1]Department of Biology, University of Central Arkansas, Conway, Arkansas

[2]Department of Biomedical Physiology and Kinesiology, Simon Fraser University, Burnaby, British Columbia, Canada

[3]Department of Psychology, Vanderbilt University, Nashville, Tennessee

[4]Systems Neuroscience Institute, University of Pittsburgh School of Medicine, Pittsburgh, Pennsylvania

[5]Center for Neuroscience, University of California, Davis, California

[6]Department of Psychology, University of California, Davis, California

Correspondence
Leah Krubitzer, Center for Neuroscience, 1544 Newton Court, Davis, CA 95618.
Email: lakrubitzer@ucdavis.edu

Abstract

The overarching goal of the current investigation was to examine the connections of anterior parietal area 2 and the medial portion of posterior parietal area 5 in macaque monkeys; two areas that are part of a network involved reaching and grasping in primates. We injected neuroanatomical tracers into specified locations in each field and directly related labeled cells to histologically identified cortical field boundaries. Labeled cells were counted so that the relative density of projections to areas 2 and 5 from other cortical fields could be determined. Projections to area 2 were restricted and were predominantly from other somatosensory areas of the anterior parietal cortex (areas 1, 3b, and 3a), the second somatosensory area (S2), and from medial and lateral portions of area 5 (5M and 5L respectively). On the other hand, area 5M had very broadly distributed projections from a number of cortical areas including anterior parietal areas, from primary motor cortex (M1), premotor cortex (PM), the supplementary motor area (SMA), cortex on the medial wall, and from posterior parietal areas 5L and 7b. The more restricted pattern of connections of area 2 indicates that it processes somatic inputs locally and provides proprioceptive information to area 5M. 5M, which at least partially overlaps with functionally defined area MIP, receives inputs from somatosensory (predominantly from area 2), posterior parietal and motor cortex, which could provide the substrate for representing multiple coordinate systems necessary for planning ethologically relevant movements, particularly those involving the hand.

KEYWORDS
Area 2, frontal parietal, grasping, hand use, networks, posterior parietal cortex, reaching

1 | INTRODUCTION

There are a number of features that distinguish primates from other mammals. One is the evolution of the hand, which in some primates including humans, allows for a variety of complex digit manipulations and grips (Almecija & Sherwood, 2017). A second feature is the expansion of the neocortex, particularly posterior parietal cortex (PPC; (Chaplin, Rosa, & Yu, 2017; Glasser et al., 2016; Glasser, Goyal, Preuss, Raichle, & Van Essen, 2014)), which contains multiple areas devoted to planning and executing behaviors involving the hands ((Goldring & Krubitzer, 2017; Kaas & Stepniewska, 2016) for review).

One of the traditional divisions of posterior parietal cortex is Brodmann's area 5 (Brodmann, 1909), which is a large architectonically defined area that includes the rostral bank of the intraparietal sulcus (IPS), the superior parietal lobule, and continues onto the medial wall. Area 5 has been subdivided into multiple cortical areas by different investigators (Figure 1). However, there are only a few studies that directly relate architectonic subdivisions with studies of connections or with studies that examined the electrophysiological properties of neurons. Previously, we examined the functional organization of the rostral bank of the IPS utilizing electrophysiological recording techniques, including Brodmann's area 5 (Seelke et al., 2012), and found that this large region contained at least two distinct areas: a lateral area (5L), and a more medial area, termed here area 5M (Figure 1). We proposed that area 5M at least partially overlaps with previously described

Jeffrey Padberg and Dylan F. Cooke co-first authors.

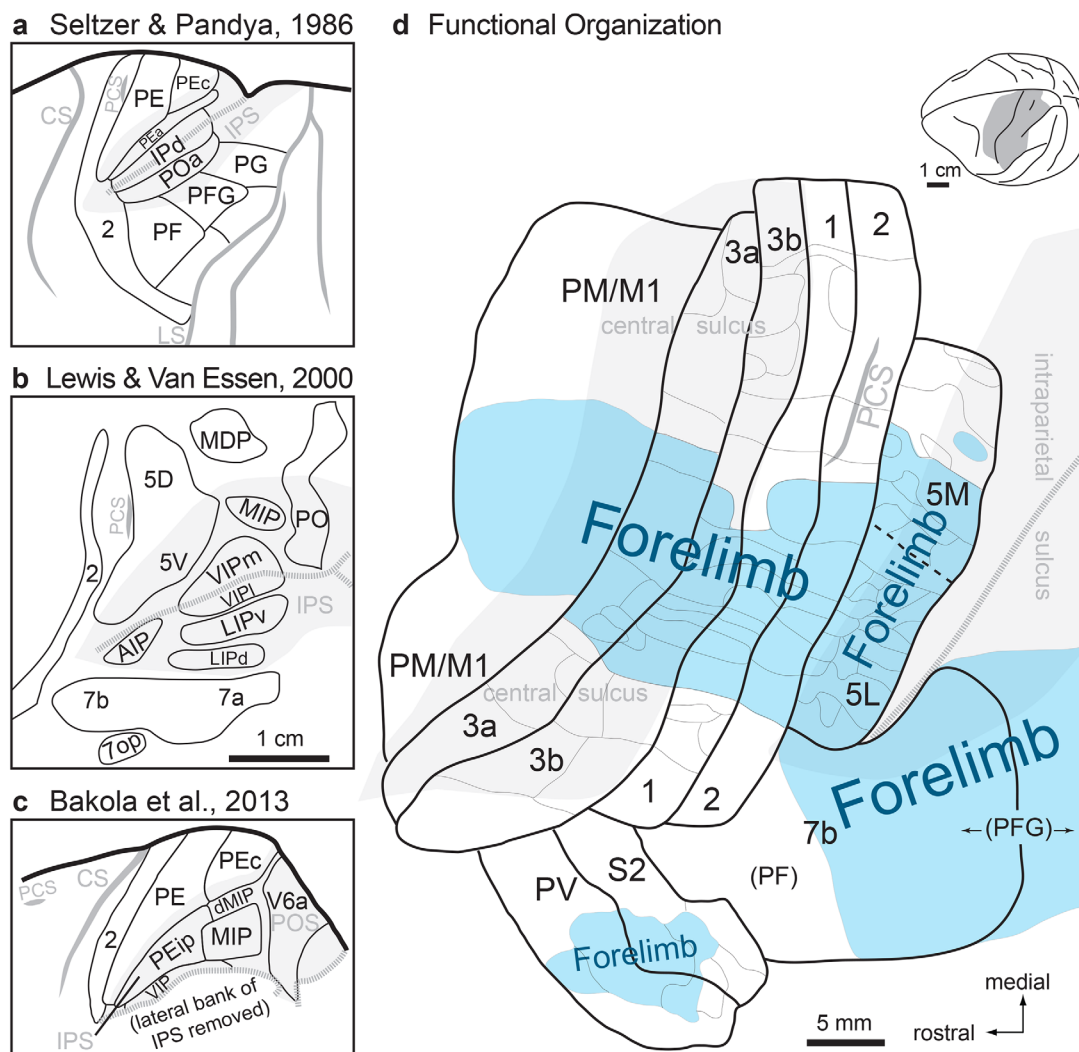**a** Seltzer & Pandya, 1986   **d** Functional Organization

FIGURE 1 Architectonic (a–c) and functional subdivisions (d) of parietal, motor and posterior parietal cortex in macaque monkeys. Commonly used architectonic subdivisions of parietal cortex include those of Seltzer and Pandya ((Seltzer & Pandya, 1986); (a) and Lewis and Van Essen ((Lewis & Van Essen, 2000); (b). We make comparisons to connections reported by Bakola and colleagues ((Bakola et al., 2013); (c). Opened sulci are shaded light gray with the fundi indicated by thick, dashed, darker-gray lines. Closed sulci are shown as solid, dark gray lines. Black lines depict areal borders. Thin black lines in (d), are functional borders of individual body part representations. Fore-limb representations are shaded light blue. Gray shading on inset brain in (d) shows the approximate location of cortex depicted. A number of studies have defined cortical areas in parietal, motor and posterior parietal cortex using electrophysiological or intracortical microstimula-tion techniques and related their results to cortical architecture. While anterior parietal and lateral sulcus fields have a somatotopic organi-zation, posterior parietal fields have a fractured topography, much like motor and premotor cortex. In addition, with few exceptions, area 5L contains only representations of deep receptors of the hand, forelimb and shoulder. Area 5M is dominated by these representations as well, but does have a relatively small amount of space devoted to representation of the lower extremities and face (Seelke et al., 2012). Neurons in the inferior parietal lobule (7b or PF + PFG) are organized by motor acts or action goals. In the present investigation, we combine func-tional mapping with architecture to define the location of our injection sites as well as the location of retrogradely labeled cells. These maps of different cortical areas defined in previous studies allow us to accurately infer the body part representations in which the labeled neurons were found. Much of this figure is redrawn from (Seelke et al., 2012). Primary data for these maps comes from (Godschalk, Mitz, van Duin, & van der Burg, 1995; Krubitzer et al., 1995; Krubitzer et al., 2004; Nelissen & Vanduffel, 2011; Nelson et al., 1980; Pons et al., 1985; Rozzi et al., 2008; Seelke et al., 2012). See Table 1 for abbreviations

cortical fields defined architectonically (e.g., PE/5D) and functionally (e.g., MIP; (Colby & Duhamel, 1991, 1996; Klam & Graf, 2006), see (Seelke et al., 2012) for review). Unlike the complete body maps found in anterior parietal fields (3a, 3b, 1, and 2), 5L and 5M are dominated by the forelimb and hand representation, and the maps are fractured or discontinuous, much like the organization of motor cortex (Cooke,

Padberg, Zahner, & Krubitzer, 2012; Gould, Cusick, Pons, & Kaas, 1986; Schieber, 2001).

Since the seminal electrophysiological recording studies in awake behaving monkeys of Vernon Mountcastle (Mountcastle, Lynch, Geor-gopoulos, Sakata, & Acuna, 1975), posterior parietal cortex has been implicated in reaching and grasping. Single unit recording studies in the

TABLE 1 Abbreviations

Sulci

AS	Arcuate sulcus
CgS	Cingulate sulcus
CS	Central sulcus
IPS	Intraparietal sulcus
LS	Lateral sulcus
PCS	Postcentral sulcus
POS	Parieto-occipital sulcus
sPrCS	Superior precentral sulcus
STS	Superior temporal sulcus

Cortical Fields / Regions

1		Area 1; cutaneous representation caudal to 3b
2		Area 2; representation of deep receptors caudal to area 1
3a		Area 3a; somatosensory field rostral to 3b
3b		Area 3b, primary somatosensory area, S1
5D		Area 5, dorsal division; Figure 1B
5V		Area 5, ventral division; Figure 1B
5L		Area 5, lateral division; from Seelke et al. (Seelke et al., 2012)
5M		Area 5, medial division; overlaps MIP
7a		Area 7a
7b		Area 7b
7op		Operculor area 7; Figure 1B
AIP		Anterior intraparietal area
DM		Dorsomedial visual area
dMIP		Dorsocaudal strip of the medial intraparietal area from Bakola et al. (Bakola et al., 2013); Figure 1C
FEF		Frontal eye fields
IPd		Intraparietal depth area; Figure 1A
LIP		Lateral intraparietal area
	LIPd	LIP, dorsal division; Figure 1B
	LIPv	LIP, ventral division; Figure 1B
M1		Primary motor cortex
MDP		Medial dorsal parietal area; Figure 1B
MIP		Medial intraparietal area
MST		Middle superior temporal visual area
MT		Middle temporal visual area
PE		Parietal area E; mostly coextensive with Brodmann's (1909) original area 5; Figure 1A
	PEa	Parietal area E, anterior (not part of Seltzer and Pandya's (Seltzer and Pandya, 1986) PE); Figure 1A
	PEc	Parietal area E, caudal (not part of Seltzer and Pandya's (Seltzer and Pandya, 1986) PE); Figure 1A
PEip		Parietal area E, intraparietal from Bakola et al. (Bakola et al., 2013); Figure 1C
PF		Parietal area F; overlaps 7b; Figure 1A,D
PFG		Parietal area FG; (transitional area between PF and PG) from Seltzer and Pandya (Seltzer and Pandya, 1986); may straddle 7a/7b border; Figure 1A,D
PG		Parietal area G; overlaps 7a; Figure 1A
PM		Premotor cortex
PMd		dorsal PM
PMv		ventral PM
PO		Parietal occipital area (approximately V6 + V6a); Figure 1B
POa		Area POa (not part of PO); overlapping LIP and AIP; Figure 1A
PPC		Posterior parietal cortex
PR		Parietal rhinal area
PRR		Parietal reach region
PV		Parietal ventral area
S1		Primary somatosensory cortex
S2		Secondary somatosensory cortex
SMA		Supplementary motor cortex
V2		Second visual area
V3		Third visual area
VIP		Ventral intraparietal area
	VIPl	VIP, lateral division; Figure 1B
	VIPm	VIP, medial division; Figure 1B
VS		Ventral somatosensory area; part of the S2 complex from Krubitzer et al. (Krubitzer et al., 1995)

Neuroanatomical Tracers

CTB	Cholera toxin B subunit
DY	Diamidino Yellow
FE	Fluoro-emerald
FR	Fluoro-ruby

Other

CO	Cytochrome oxidase
IM	Intramuscular

TABLE 2 Cases and injections

Case/species	Tracer	Injection location	Receptive field at injection location
A *M. mulatta*	0.6 ul 1% CTB	5M	dorsal digit 1, ventral wrist, radial hand
	0.5 ul 2% DY	2	palm: hypothenar pad, thenar pad, insula
B *M. mulatta*	0.3 ul 7% FR	2	not mapped
C *M. radiata*	0.6 ul 1% CTB	5M	hypothenar pad
D *M. mulatta*	0.4 ul 7% FR	5L	hand
	0.4 ul 7% FE	5M	forelimb
E *M. mulatta*	0.3 ul 7% FE	5M	unresponsive

lateral portion of area 5 indicate that neurons fire maximally during a reaching task before the target object is contacted by the hand (Gardner, Babu, Ghosh, Sherwood, & Chen, 2007; Gardner, Babu, Reitzen, et al., 2007), and modulate their activity depending on how and when the hand is used in a grasp (Chen, Reitzen, Kohlenstein, & Gardner, 2009). For medial portions of area 5, including MIP, it appears that multiple frames of reference (e.g., body-centered, eye-centered) share a common coordinate system in that neurons in this region are heterogeneously tuned to multiple types of sensory inputs (e.g., (McGuire & Sabes, 2009, 2011)). Such modality-independent representations compute the position of the hand/body and the object to be acquired, depending on the available sensory input, to plan and execute precise movements.

Area 2 is an anterior parietal field just rostral to area 5 and contains neurons responsive to cutaneous stimulation and stimulation of proprioceptors (Hyvarinen & Poranen, 1978a,b; Iwamura, Tanaka, Sakamoto, & Hikosaka, 1993; Pons, Garraghty, Cusick, & Kaas, 1985). Recent studies indicate that neurons in area 2 respond to both passive and active movement of the arm (London & Miller, 2013) and that it is involved in distinguishing internally generated movements from movements due to execution errors; thus, providing proprioceptive feedback for movement correction. In addition, neurons in area 2 are tuned for curved shapes (Yau, Connor, & Hsiao, 2013) indicating that area 2 is involved in stereognosis or haptic shape perception (see Delhaye, 2017; Yau et al., 2013).

Recent work in our laboratory in macaque monkeys also supports the possibility that area 2 and portions of area 5 may be directly involved in motor control of the hands, since intracortical microstimulation evokes movements of the hand and digits from these areas (Baldwin, Cooke, Goldring, & Krubitzer, 2017). The goal of the current study was to examine the overall pattern of cortical connections of areas 5M and 2 to determine the extent to which each is connected with somatosensory, posterior parietal areas and motor cortex, and the underlying anatomical substrate for their potential roles in planning and providing feedback for reaching and grasping movements.

2 | METHODS

One adult bonnet macaque monkey (*Macaca radiata*; Monkey C) and four adult rhesus macaque monkeys (*Macaca mulatta*) were used to study the cortical connections of posterior parietal area 5M and anterior parietal area 2 (Table 2). All experimental procedures were approved by the UC Davis or Vanderbilt Institutional Animal Care and Use Committees (IACUCs) and adhered to National Institutes of Health guidelines.

At the start of each experiment, animals were anesthetized with an intramuscular (IM) injection of ketamine hydrochloride (20–35 mg/kg) and then intubated and cannulated. Anesthesia was then maintained with 1.5–2% isoflurane. Animals were also administered atropine (0.4 mg/kg, IM). All surgeries were performed under standard sterile conditions and antibiotics were administered postoperatively to prevent infection. Once anesthetized, topical lidocaine (2%) was applied to the external ear canals and the animals were placed in a stereotaxic frame. The skin was cut, the temporal muscle retracted, and a craniotomy was made over parietal and posterior parietal cortex. The dura was cut and retracted to expose anterior parietal cortex and the IPS, and a digital image of the exposed neocortex was taken so that injection sites and electrode tracks could be marked relative to the vasculature. Throughout the procedure, respiration rate, heart rate, temperature, blood oxygenation and expired pCO$_2$ were continuously monitored. In addition, to maintain hydration, a lactated Ringer's solution was administered intravenously (6–10 ml/kg/h).

Five of the injections were made under electrophysiological guidance. Extracellular recordings were made from depths corresponding to layer 4, using tungsten microelectrodes designed to record extracellularly from single units and clusters of neurons (FHC, Inc., Bowdoin, ME; "no zap," or A-M Systems, Sequim, WA; 1–5 MΩ) lowered with a hydraulic microdrive (David Kopf Instruments, Tujunga, CA). At each recording site, neural responses to somatosensory stimulation (consisting of light taps, displacement of hairs, brushing of skin, hard taps and manipulation of muscles and joints) were tested using a handheld probe. Neural activity was monitored through a loudspeaker and viewed on a computer monitor during the experiment. Electrode penetrations were marked on high resolution digital images of the brain. The goal was to identify receptive fields for neurons at the center of the injection site. In cases in which injections sites were determined under electrophysiological guidance, injections were in representations of the hand and/or distal forelimb.

Once receptive fields for neurons at a recording/injection site were identified, a Hamilton syringe was used to inject anatomical

tracers in each field, including 0.3–0.4 μl Fluoro-emerald (FE; Molecular Probes, Eugene, OR; 7% in distilled water), 0.3–0.4 μl Fluoro-ruby (FR; Molecular Probes, Eugene, OR; 7% in distilled water), 0.5 μl of Diamidino Yellow (DY; Sigma, St. Louis, MO, 2% in 0.1 M phosphate buffer), and 0.6 μl of Cholera Toxin Subunit-B (CTB; 1% in distilled water). For details of the anatomical tracers used, concentration, amounts injected and representation injected, see Table 2. Injections in area 2 were centered in layer 4 and encompassed all cortical layers. Injections in area 5M were made at a similar depth near the lip of the IPS or into the rostral bank of the IPS. After the injections were made, the cortex was covered with a sterile contact lens or absorbable gelatin film, the skull was closed with a cap of dental cement, and the skin was sutured. After recovery from anesthesia, animals were returned to their home cage. Oxymorphone (0.15 mg/kg, IM) was administered immediately following surgery to relieve pain or any discomfort. Buprenorphine (0.03 mg/kg, IM) was administered twice daily for 48 hr. Ketoprofen (2 mg/kg, IM) was administered once a day for 5 postoperative days including the day of surgery. To prevent infection, enrofloxacin (5 mg/kg IM) was administered once a day for 10–14 postoperative days including the day of surgery. Each day a 28-item pain score was assessed. If scores exceeded 1, the facility veterinarian was consulted and care was adjusted.

2.1 | Histological processing of tissue

Following a 9- to 14-day recovery period, the animals were given a lethal dose of sodium pentobarbital and perfused through the heart with phosphate buffered saline followed by 2% paraformaldehyde in buffered saline and 2% or 4% paraformaldehyde with 10% sucrose. The brain was removed and the cortex separated from the thalamus. The cortex was blocked and flattened as described previously (Seelke et al., 2012; Stepniewska, Fang, & Kaas, 2005), held between two glass slides, and stored overnight in 30% sucrose at 3°C. The cortex was cut parallel to the surface at a thickness of 40 or 50 μm on a freezing microtome. Depending on the tracers used, alternate sections were mounted unstained for fluorescence microscopy, processed to reveal CTB (Bruce & Grofova, 1992), processed for myelin (Gallyas, 1979) or for cytochrome oxidase (CO (Wong-Riley, 1979)).

The flattening technique has been used in macaque monkeys by our own (e.g., (Gharbawie, Stepniewska, Qi, & Kaas, 2011)) and other laboratories (e.g., (Sincich, Jocson, & Horton, 2010)) to examine the areal patterns of cortical connections. While laminar information (and distribution of labeled cells across layers) is largely lost in tangential sections, the entire pattern of connections can be appreciated in our final reconstructions. Cortical field boundaries are generated from an entire series of sections so that accurate designation of cortical field boundaries is possible.

2.2 | Data analysis

For each section in the entire series, injection sites and neurons labeled with fluorescent tracers and CTB (Figure 2) were plotted with a high-resolution fluorescence microscope coupled to a Neurolucida system
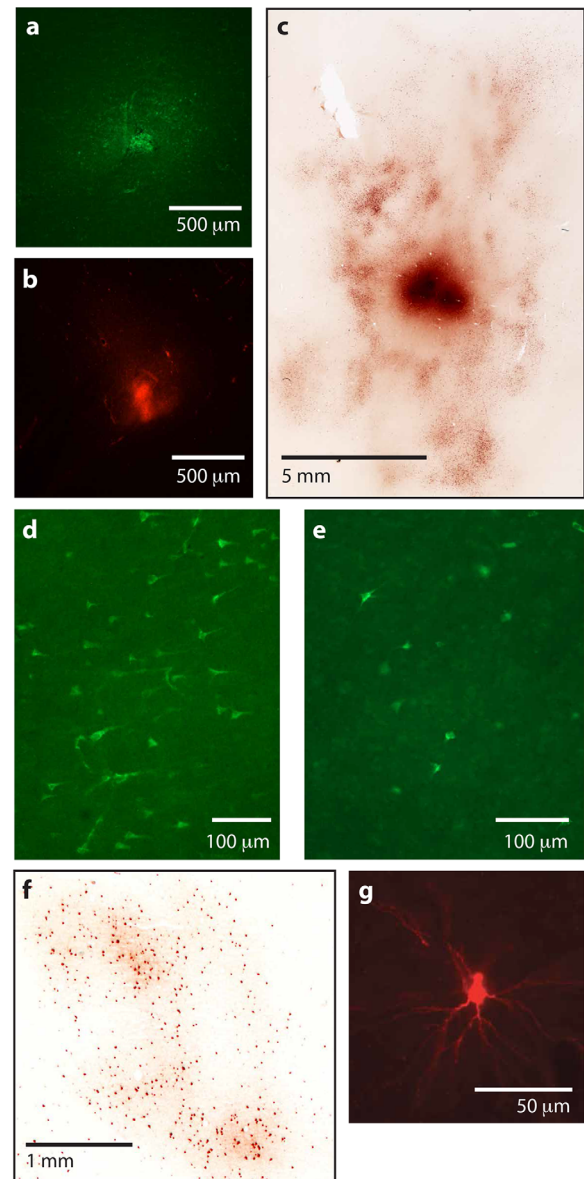

FIGURE 2 Injection sites and labeled neurons. Injection sites of Fluoro-emerald (FE) in area 5M (a) and Fluoro-ruby (FR) in 5L (b) in Monkey D. Injections are small, but reconstructions through the entire series of sections indicate that the injection site encompassed all cortical layers. (c) An injection of CTB in area 5M in Monkey A and surrounding patches of labeled neurons both within 5M and in adjacent cortical areas. Following an FE injection in area 5M, retrogradely labeled cells in area 2 (d) are more densely packed than those found at adjacent mediolateral levels in area 1 (e). (f) Labeled cells in S2 following an injection of CTB. (g) A cell retrogradely labeled with FR following an injection in area 2. In all cases the signal to noise ratio of these cells was high

(MBF Bioscience, Inc., Williston, VT) or reconstructed on a fluorescent microscope using an X/Y stage encoding system (MD Plot, Minnesota Datametrics, St. Paul, MN) connected to a computer. Because we reconstructed the entire series of sections, for each case we confirmed that the injection site included all cortical layers. Tissue outline, blood vessels and other landmarks were marked on the plots for alignment with architectonic sections. The boundaries of cortical fields were

determined for an entire series of sections using a camera lucida attached to a stereomicroscope to draw individual sections that were stained for myelin. The architectonic borders were directly aligned to sections in which the injection site and retrogradely labeled cells were plotted by matching blood vessels, sulci and tissue artifacts. All individual reconstructions were combined into a comprehensive reconstruction by aligning blood vessels, injection sites and other artifacts using Adobe Illustrator CS6 (Adobe Systems Inc.: United States). Light field images of myelin-stained tissue (Figure 3) were made with a Nikon Multiphot (Tokyo, Japan) with a Phase One PowerPhase FX+ scan back (Global Manufacturing, Louisville, CO). In most cases, the center of the injection site was determined under electrophysiological guidance. However, myeloarchitectonic boundaries were used to determine if injections sites were restricted to the field of interest.

This comprehensive reconstruction contained the injection site, labeled cell bodies and architectonic boundaries of cortical fields. These data were used to quantify the percentage of labeled cells in each cortical area as follows: Markers representing labeled cells in Illustrator CS6 were segregated according the architectonic boundaries such that the cell markers of each cortical field were placed in separate sublayers. All of the cell markers for a given cortical field were then selected and counted using the Illustrator software. Cell counts for each cortical field were divided by the total number of labeled cells within the hemisphere (Table 3). In this way, data across cases with varying injection sizes were normalized and could be compared. Only those labeled cells outside of the injection halo were included in this quantification. Counts of all such labeled cells in each cortical field/region for each case can be found Table 3.

3 | RESULTS

Here we describe the ipsilateral corticocortical projections to areas 2 and 5M. In one case (Monkey D) we missed our target area (5M) and injected 5L. Because we have only one injection in one animal in area 5L, we illustrate this injection, but only briefly describe these results. Two injections were made in area 2 in two different animals, and 4 injections were made in area 5M in four animals (see Table 2). Two animals had injections in more than one field: Monkey A, in areas 2 and 5M, and Monkey D in areas 5M and 5L. In the following results, we first describe the architectonic boundaries of a number of fields in anterior parietal, posterior parietal, lateral sulcus and frontal cortex. This is followed by descriptions of connections of areas 2 and 5M.

3.1 | Architecture of the neocortex

Cortex was flattened, sectioned tangential to the pial surface and stained for myelin. Since individual sections do not contain all of the boundaries of all of the fields of interest, the entire series of sections was used to determine the architectonic boundaries. Here we briefly describe the cortical areas injected with anatomical tracers and the fields in which retrogradely labeled neurons were located, since the appearance of most of these fields has been previously described by our own and other laboratories for the macaque monkey (Krubitzer,
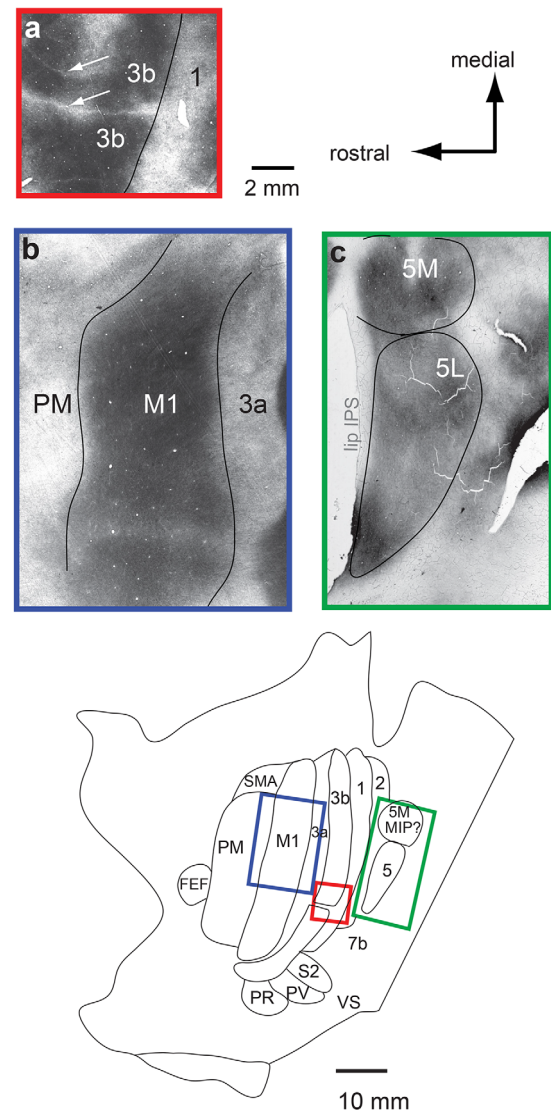

FIGURE 3 Light field images of flattened cortex cut tangentially to the pial surface and stained for myelin. The location of these panels is color coded on the schematic flattened cortex at bottom. (a) Area 3b is distinguished by its dark myelination with major body part representations separated by myelin-light zones (arrows mark the hand/face border, bottom, and individual digit representations, top). Area 1 is immediately adjacent and stains lightly for myelin. (b) The primary motor area (M1) is darkly myelinated and flanked rostral and caudally by more lightly myelinated fields (areas PM and 3a respectively. (c) Area 5L is a moderately to darkly myelinated wedge of cortex that resides almost completely on the rostral bank of the IPS, just lateral to area 5M, while area 5M is a darkly myelinated oval of cortex located partly on the dorsolateral surface of the cortex, just caudal to the PCS and partly on the rostral bank of the IPS, just medial to area 5L. Due to an uneven flattening of the sulcal crown compared to areas on sulcal walls and the adjacent dorsolateral cortex, the sulcal lip often stains lightly, giving the erroneous impression of a cortical field boundary. (Regardless of the plane of section used, discontinuities here may have contributed to previous divisions of area 5/PE at the medial lip of the IPS ((Bakola et al., 2013); Figure 1a–c; (Lewis & Van Essen, 2000; Seltzer & Pandya, 1986)). Boundaries of cortical fields shown in the subsequent reconstructions are obtained by reconstructing the entire series of sections. Conventions as in previous figures

TABLE 3 Quantification of labeled neurons in cortical fields following injections in Areas 2, 5M, and 5L

Location of cells	Area 2 injections						Area 5M injections												Area 5L	
	Monkey A		Monkey B		Mean	STD	Monkey A		Monkey C		Monkey D		Monkey E		Mean	STD			Monkey D	
	cells	%	cells	%	%	%	cells	%	cells	%	cells	%	cells	%	%	%			cells	%
SMA	0	0.00	0	0.00	0.00	0.00	2245	1.61	1720	4.54	76	1.00	12	0.77	1.98	1.74			117	2.04
PM	5	0.03	6	0.44	0.23	0.29	2622	1.88	1138	3.00	205	2.69	63	4.05	2.90	0.90			145	2.53
M1	401	2.34	12	0.88	1.61	1.03	5964	4.27	3147	8.30	667	8.74	24	1.54	5.71	3.43			373	6.51
3a	1303	7.60	16	1.17	4.38	4.55	2688	1.93	215	0.57	209	2.74	15	0.96	1.55	0.98			627	10.95
3b	2418	14.10	160	11.69	12.89	1.71	2482	1.78	2038	5.38	135	1.77	9	0.58	2.38	2.08			687	11.99
1	2241	13.07	306	22.35	17.71	6.56	11196	8.02	952	2.51	256	3.35	30	1.93	3.95	2.78			1165	20.34
2	8740	50.97	362	26.44	38.71	17.34	32846	23.54	4218	11.13	902	11.81	84	5.40	12.97	7.61			514	8.97
med wall	0	0.00	0	0.00	0.00	0.00	1631	1.17	789	2.08	151	1.98	55	3.53	2.19	0.98			9	0.16
med parietal	0	0.00	1	0.07	0.04	0.05	3594	2.58	1475	3.89	942	12.34	55	3.53	5.59	4.54			22	0.38
5M	929	5.42	12	0.88	3.15	3.21	48629	34.85	14155	37.35	2801	36.69	735	47.24	39.03	5.57			444	7.75
5L	896	5.23	137	10.01	7.62	3.38	13722	9.83	5696	15.03	743	9.73	389	25.00	14.90	7.17			1146	20.01
7b	14	0.08	42	3.07	1.57	2.11	4013	2.88	1212	3.20	336	4.40	61	3.92	3.60	0.69			373	6.51
S2	173	1.01	305	22.28	11.64	15.04	3389	2.43	568	1.50	72	0.94	15	0.96	1.46	0.70			1	0.02
Other	28	0.16	10	0.73	0.45	0.40	4503	3.23	580	1.53	140	1.83	9	0.58	1.79	1.10			105	1.83
Total	17148	100.00	1369	100.00			139524	100.00	37903	100.00	7635	100.00	1556	100.00					5728	100.00

Huffman, Disbrow, & Recanzone, 2004; Nelson, Sur, Felleman, & Kaas, 1980; Padberg et al., 2010; Pons & Kaas, 1986; Rothemund, Qi, Collins, & Kaas, 2002; Seelke et al., 2012).

Some areas are particularly distinct in this type of tissue preparation. For example, the primary somatosensory area (S1 or area 3b) is a thin, L-shaped field located along the entire caudal bank of the central sulcus (CS), and sometimes wrapping onto the postcentral gyrus. Area 3b stains very darkly for myelin, and in favorable preparations, individual body part representations are separated by myelin-light zones, giving the field a heterogeneous appearance. This is particularly true for the hand/face border (Figure 3a). Moving caudally, area 1 is distinguished from area 3b by its light to moderate myelination, while area 2 is more darkly myelinated. Immediately adjacent to the caudal boundary of area 2 are two distinct fields that have been defined both functionally and architectonically. One is area 5M, which abuts the medial half of area 2. This field is a moderately myelinated oval of cortex that resides partly on the dorsolateral surface of cortex, just caudal to the postcentral sulcus (PCS), and partly on the anterior bank of the IPS (Figure 3c). The second field on the caudal border of area 2 is area 5L, which adjoins the lateral border of 5M. It is a wedge-shaped field that is somewhat more densely myelinated than area 5M (Figure 3c).

Rostral to area 3b, there are several distinct fields. Immediately adjacent to the rostral border of area 3b is area 3a, a moderately myelinated field that resides mostly on the rostral bank of the CS (Figure 3b). As reported previously, however, the position of fields in the CS can vary, so that in some individuals, area 3a straddles the fundus, while in others it is completely restricted to the rostral bank (Krubitzer et al., 2004); examples of both configurations are illustrated in our figures. Just rostral to area 3a is the densely myelinated primary motor cortex (M1) followed by the moderately myelinated premotor cortex (PM; Figure 3b). PM has been subdivided into functional and structural subdivisions (e.g., PMd and PMv; Matelli, Luppino, & Rizzolati, 1985; Preuss, Stepniewska, & Kaas, 1996) but these are not distinct in our preparations. Areas PM, M1, 3a, 3b, 1, and 2 form long mediolateral strips that run parallel to the CS. Medial to M1 and PM, the moderately myelinated SMA resides partially on the dorsolateral surface of the neocortex and then wraps onto the medial wall.

Finally, there are several fields in or near the lateral sulcus that have been defined both functionally and architectonically (Disbrow, Litinas, Recanzone, Padberg, & Krubitzer, 2003; Krubitzer, Clarey, Tweedale, Elston, & Calford, 1995). Most notable are areas S2 and PV. S2 is a moderately myelinated field that abuts the lateral border of both areas 1 and 3b. Rostral to this is the lightly myelinated PV, which also adjoins the lateral border of area 3b. Caudal to S2 and lateral to area 2 is the lightly myelinated area 7b. 7b has been subdivided into several functional and architectonic subdivisions (Gregoriou, Borra, Matelli, & Luppino, 2006; Rozzi et al., 2006; Rozzi, Ferrari, Bonini, Rizzolatti, & Fogassi, 2008), but these are not distinct in our preparations Most of the labeled cells found in area 7b were in the rostral portion of this field, which corresponds to area PF and possibly portions of PFG as described by Seltzer and Pandya (Seltzer & Pandya, 1986) and Rozzi and colleagues ((Rozzi, Ferrari, Bonini, Rizzolatti, & Fogassi, 2008); Figure 1).

3.2 | Cortical connections of area 2

Area 2 was injected in two monkeys. In Monkey A, a DY injection was placed in the representation of the glabrous hand (Figure 4; see Table 2 for details on tracers and body part representation injected). In Monkey B, the receptive field of neurons in the location of the injection of FR was not determined (Figure 5). Overall patterns of connectivity from these two cases were similar, but there was some variability in the density of connections from different fields. This may have been due to differences in the representation that was injected in each case. In both cases, the densest projections were intrinsic, from labeled cells surrounding the injection location in area 2 (Figure 6; mean across 2 cases = 38.7% of total label in hemisphere; see Table 3 for complete cell counts for all cases and injections). Dense projections were also observed from somatosensory areas 1 (17.7%) and 3b (12.9%) in the expected location of the hand representation (Figure 1). In one case, moderate projections from homotopic locations were observed from area 3a (7.6% in Monkey A; Figures 4 and 6), while in the second case, very light distributed projections were observed from area 3a (1.2% in Monkey B; Figures 5 and 6). While the absolute number of labelled cells in Monkey A was greater than in Monkey B, by percentage of all labeled cells observed in the hemisphere, the projections from M1 were relatively sparse in both cases (2.3% in Monkey A, .9% in Monkey B, mean = 1.6%).

Projections were observed from middle portions of the second somatosensory area (11.6%; S2; Figures 4–6) in the approximate location of the hand representation in this field (Figure 1d), but the density of labeling varied. In both cases, light projections were also observed from VS (0.4%) and 7b (1.6%). Finally, two posterior parietal areas projected to area 2. The first was the lateral portion of area 5 (area 5L). Projections were moderate in both cases (7.6%); in one case, projections were mostly clustered along the anterior medial portion of 5L (Figure 4) and in the other case they were scattered along the mediolateral extent of the field. Since area 5L has a fractured and variable somatotopy and only contains representations of the digits, hand and forelimb, it was not possible to estimate if projections were from homotopic representations. Area 5M also projected to area 2. In one case these projections were moderate (Figure 4) and in the second case, projections were sparse (Figure 5).

3.3 | Cortical connections of 5M

The ipsilateral cortical connections of area 5M were examined in 4 cases (Figures 7–9; Monkey E, not shown). In all cases, injections were centered in the representation of the hand and/or forelimb (Figures 7–9) or in the expected location of this representation (Monkey E); in three of these cases the injection site was restricted to area 5M (Figures 7 and 9; Monkey E, not shown) and in one case the injection spread slightly into area 2 (Figure 8; see Table 2 for details on tracers injected and body part representation injected). In two animals, CTB was injected into area 5M (Figures 7 and 8), and in two animals FE was injected into area 5M (Figure 9; Monkey E, not shown). The patterns and density of labeling were remarkably similar for all cases (Figure 6; also see Table 3).
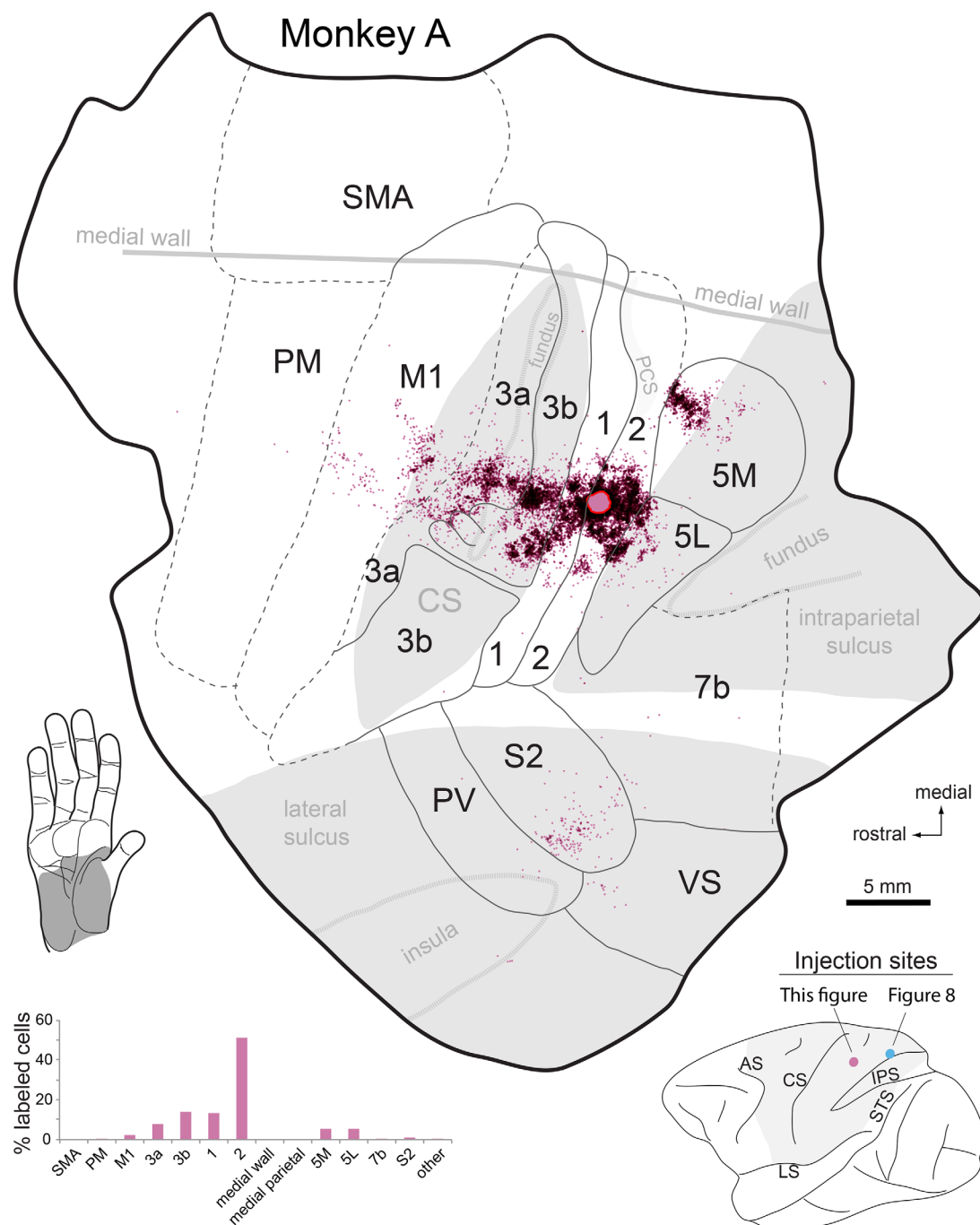
FIGURE 4 A reconstruction of an injection of Diamidino Yellow in area 2 in Monkey A. This block is one of three that together encompassed the entire cortical sheet. Labeled cells were not observed in other blocks. This block was taken from the location depicted in gray on the whole brain illustrated on the lower right. In this case, an injection (pink circle outlined in red) was centered in the representation of the palm. Very dense patches of retrogradely labeled cell bodies are observed intrinsically in area 2, and moderate to dense patches are found in topographically matched representations in areas 1, 3b, and 3a. Labeled cells are also observed in the estimated location of the hand representation in M1. Moderate clusters of labeled cells are observed in area 5M and 5L and sparse label is observed in S2. Small pink dots mark labeled cell bodies; overlapping circles are darkened to indicate label density. Solid lines represent architectonic boundaries determined with myelin stains and dashed lines represent estimated boundaries. Opened sulci are shaded gray. The plot on the lower left represents the number of labeled cells in each area as a percentage of all the cells found in the hemisphere. Conventions as in previous figures

Intrinsic projections were extremely dense for all cases (mean across 4 cases = 39.0% of total label in hemisphere) as were projections from 5L and area 2. Labeled cells in area 5L (14.9%) were located in the medial-most portion of the field in 3 cases (Figures 7–9) and were scattered throughout 5L in the other case, Monkey E (not shown). Although the density of labeled cells in area 2 was moderate to high in
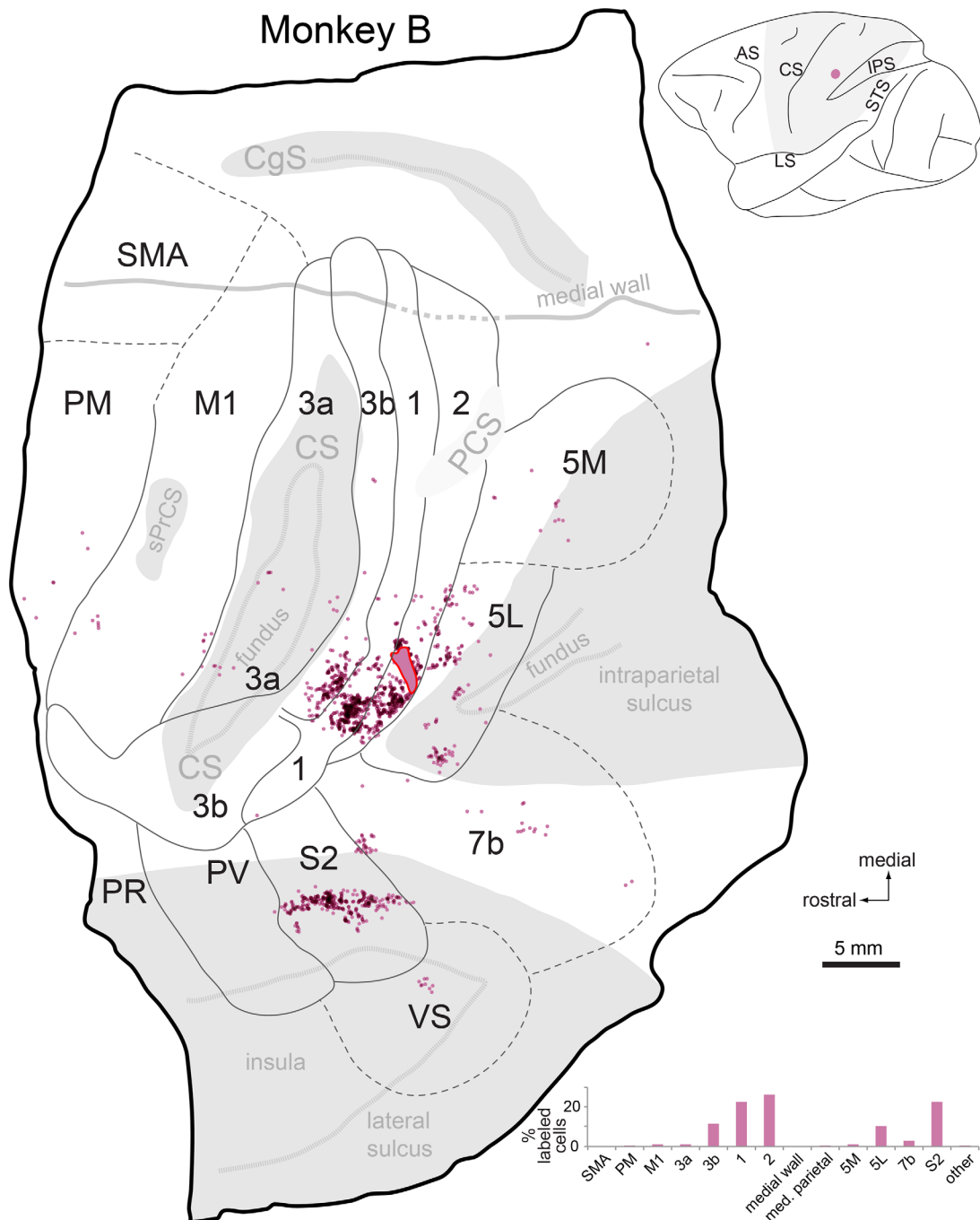
FIGURE 5 A reconstruction of a very small injection of Fluoro-ruby centered in the estimated hand representation of area 2 of Monkey B. As in the area 2 injection in Figure 4, dense labeling is found intrinsically, and in matched representations in areas 1 and 3b. Dense labeling is also observed in areas S2 and area 5L. Moderate to sparse labeling is observed in areas 3a, M1, 5M, 7b, and VS. Although the injection was made in the right hemisphere, the illustration has been left-right reversed for better comparison with other cases. Conventions as in previous figures

all cases (13.0%), the location of labeled neurons in area 2 varied between cases. In an injection in the hypothenar representation, the majority of labeled cells in area 2 were located somewhat laterally, in the expected location of the wrist/forelimb representation (Monkey C, Figure 7; Monkey E, not shown). Small patches of labeled cells were also observed medially and far laterally in area 2 in this case. An injection placed in the digit 1/wrist representation, which spread slightly

into area 2 (Monkey A, Figure 8) resulted in labeled cells in area 2 adjacent but slightly lateral to the injection in 5M, in the expected location of the distal and proximal forelimb representation. In this case, a smaller patch of label was observed laterally in area 2 near the hand and chin representations in this field. An injection placed in a slightly lateral portion of area 5M, in the representation of the forelimb, resulted in label in area 2 slightly lateral to the injection site, caudal to
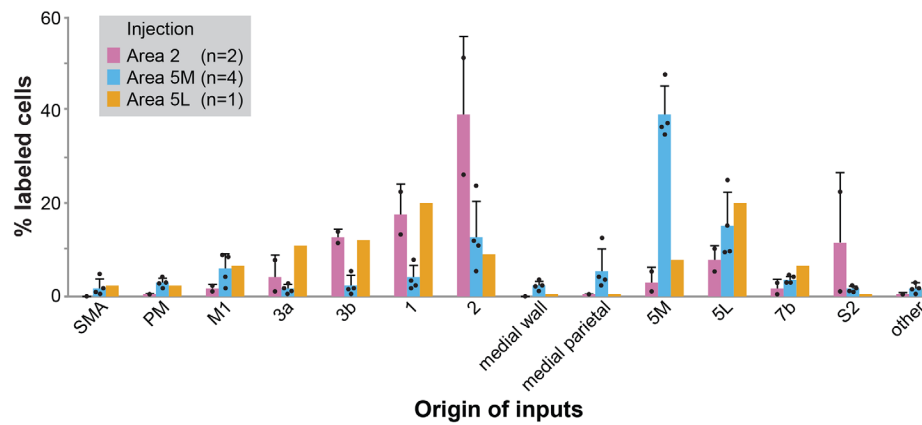
FIGURE 6 Percentages of labeled cells observed in somatosensory, motor and posterior parietal areas following injections placed in area 2 (pink; mean of two cases), area 5M (blue; mean of four cases), and area 5L (orange; one case). Black dots are values from individual cases. Most projections to area 2 are from somatosensory areas, while area 5M has dense projections from other posterior parietal fields and moderate projections from motor areas. Cell counts for these cases are in Table 3. Error bars are standard deviation

the tip of the PCS (Monkey D, Figure 9) in the expected location of the forelimb.

All injections also resulted in moderate to dense projections from cortex immediately medial to area 5M (5.6%). This region may partially overlap with portions of PRR described by other laboratories (e.g., Scherberger et al., 2003; Snyder, Batista, & Andersen, 1997, 1998); however, PRR likely contains multiple fields and has not been architectonically described. Thus, here we refer to this as the medial parietal region.

In all cases, moderate to sparse clusters of labeled neurons projecting to 5M were observed in areas 1 (4.0%), 3b (2.4%), and 3a (1.5%) at a mediolateral level similar to that observed in area 2 (Figures 6–10). It should be noted that the density of labeled cells in these anterior parietal areas was greatly reduced compared to those resulting from injections in area 2 (Figure 6). Another distinguishing feature of the connections of area 5M was the density of label observed in M1 (5.7%), compared to that produced by injections in area 2 (1.6%). In all but one case (Monkey E, not shown), large 5M injections produced moderately dense clusters of labeled cells in M1, mostly in the same mediolateral location as that of labeled cells in anterior parietal fields, in the expected location of the movement representations of the hand and arm. In all cases, but particularly in Monkey D (Figures 9–10), sparser patches of labeled cells were observed in medial and lateral locations in M1. Area 5M was also distinguished from area 2 by the presence of projections from premotor cortex, supplementary motor cortex and cortex on the medial wall around the cingulate sulcus. Projections from PM (2.9%) and SMA (2.0%) were moderate to sparse in all cases and somewhat scattered throughout the field. Labeled cells on the medial wall were also moderate to sparse (2.2%).

Finally, the second somatosensory area contained moderate to light label in all cases (1.5%). In three cases, it was localized to the middle portion of the field, in the expected location of the forelimb (Figures 7 and 8; one case not shown), and in one case it labeled cells scattered throughout the field (Figure 9). Area 5M was distinguished from area 2 by the presence of moderate projections from area 7b

(mean = 3.6%; Figures 6–9). Sparse projections were observed from areas PV in all cases and VS in all but one case (Monkey D). Area 5L was also injected in this case, and the pattern of connections was distinct from area 5M (Figures 6–9). Notably, the proportion of inputs from somatosensory areas was greater, with areas 1, 3b, and 3a together comprising over 40% of the labeled inputs to 5L. These data should be interpreted cautiously, as only one area 5L injection case was examined, however, relative to area 5M, area 5L receives fewer inputs from area 2 and medial areas.

4 | DISCUSSION

The current study demonstrates that areas 5M and 2 have distinct corticocortical connections (Figures 6 and 10a). Area 2 has a restricted pattern of extrinsic connections and is most densely connected with other somatosensory fields. Area 5M, which may partially overlap with functionally defined MIP (e.g., Colby & Duhamel, 1991; Klam & Graf, 2006; McGuire & Sabes, 2011), has a very broadly distributed pattern of projections from motor, premotor, posterior parietal and somatosensory fields (mostly from area 2). In the following discussion, we compare our results with those from other studies in macaque monkeys and with other primates.

4.1 | Connections of areas 2 and 5 in old world and new world monkeys

An early study of area 2 limited analyses to connections with anterior parietal fields and motor cortex, and most often injections were not restricted to area 2 (Jones, Coulter, & Hendry, 1978). Unlike the current study, no connections were observed with area 3b, limited and inconsistent connections were observed with area 3a, and in only one case were strong connections observed with areas 5 and motor cortex. A subsequent study also examined connections of area 2 with parietal cortex and areas in the lateral sulcus (Pons & Kaas, 1986). Although it is difficult to infer density of label from that study, the patterns of
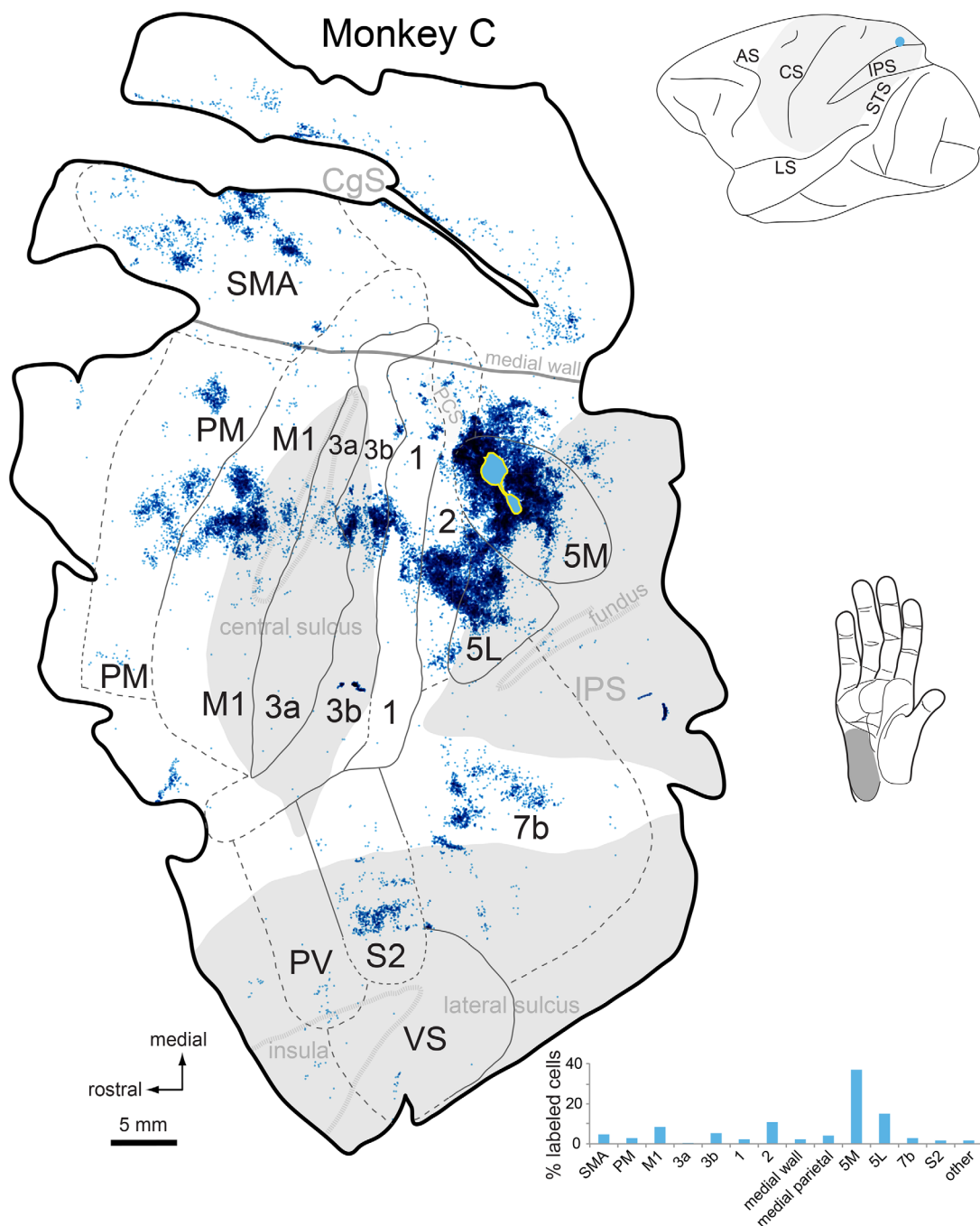
FIGURE 7 An injection of cholera toxin B subunit (CTB) in the representation of the glabrous pads of the hand in area 5M of Monkey C. Connections of area 5M differ from area 2 in several ways. In addition to dense intrinsic connections, moderate to dense projections from areas 5L, area 2, and motor cortex are observed. Less dense connections are observed with areas 3b and 1, cortex medial to area 5M ("medial parietal"), and cortex on the medial wall. Connections with 7b, premotor cortex and SMA are much denser than those observed after area 2 injections. Further, labeled cell bodies are observed on the medial wall, around the cingulate sulcus. See Figure 6 for mean percentages of labeled cells in each area. Labeled cells are marked with small blue dots. Other conventions as in previous figures

connections were like those observed in the present investigation, including projections to area 2 from anterior parietal fields, motor cortex, PPC and S2/7b. For the Pons and Kaas (Pons & Kaas, 1986) study, we counted the cells so we could better compare the density of label in the different fields with our own study (Figure 10; Table 4) and found that projection patterns and density were similar, except for the intrinsic connections which were not shown in the Pons and Kaas

study. Finally, a recent investigation examined the full patterns of corticocortical connections of area 2 in macaque monkeys (Gharbawie, Stepniewska, Qi, et al., 2011). As in the present investigation, connections were predominantly with anterior parietal areas, areas of the lateral sulcus, and area 5.

Connections of PPC in the location of Brodmann's area 5 have been examined in a few studies in macaque monkeys, but there are
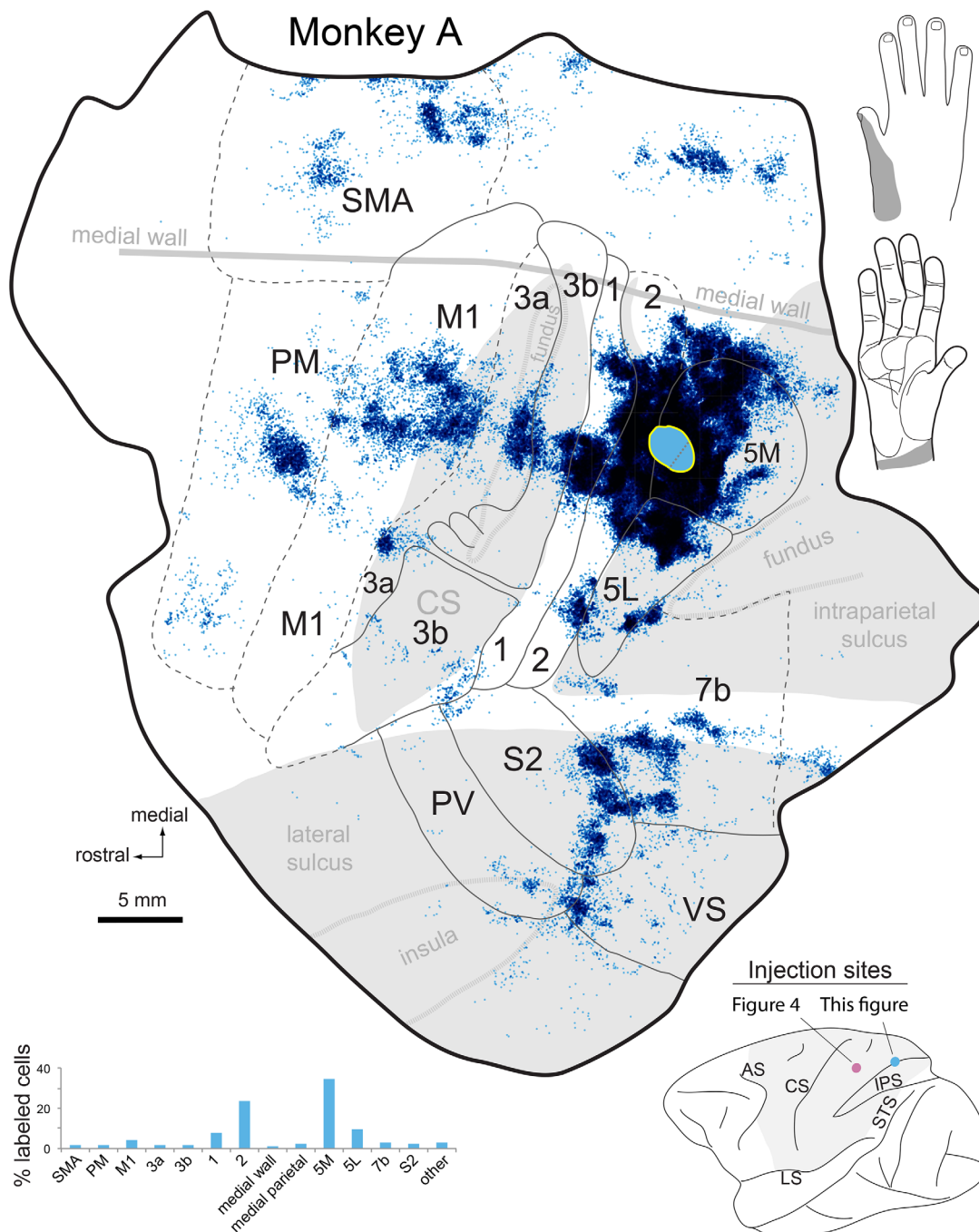
FIGURE 8 An injection of CTB centered in the representation of the palm of area 5M in Monkey A. This injection extended into the intraparietal sulcus, the lip of which is indicated with a thin, dotted gray line where it crosses the injection site. This injection spread slightly into area 2, but the overall pattern of connections is nearly identical to those observed for the area 5M injection illustrated in Figure 7. The densest labeling is intrinsic to area 5M, 5L and area 2. Moderate labeling is observed in area 1, S2, M1, and 7b. Moderate to sparse label is observed in 3a, 3b, VS, SMA, PM, medial parietal cortex, and cortex on the medial wall around the cingulate sulcus. Other conventions as in previous figures

several issues associated with each study that make direct comparisons with the present study difficult. The first is that in all but one study (Bakola, Passarelli, Gamberini, Fattori, & Galletti, 2013), the cortex was blocked and analysis was limited to a restricted region of the neocortex (Jones et al., 1978; Pons & Kaas, 1986). The second issue is that area 5 (also termed PE) was defined as a single very large field encompassing

the entire length of the rostral bank of the IPS and/or much of the dorsal cortex adjoining the IPS (e.g., (Bakola et al., 2013; Jones et al., 1978; Pons & Kaas, 1986). Recent functional studies indicate that Brodmann's area 5 is actually composed of two distinct divisions, area 5M and area 5L (Seelke et al, 2012), and single unit studies in awake behaving monkeys indicate that neural response properties differ along the
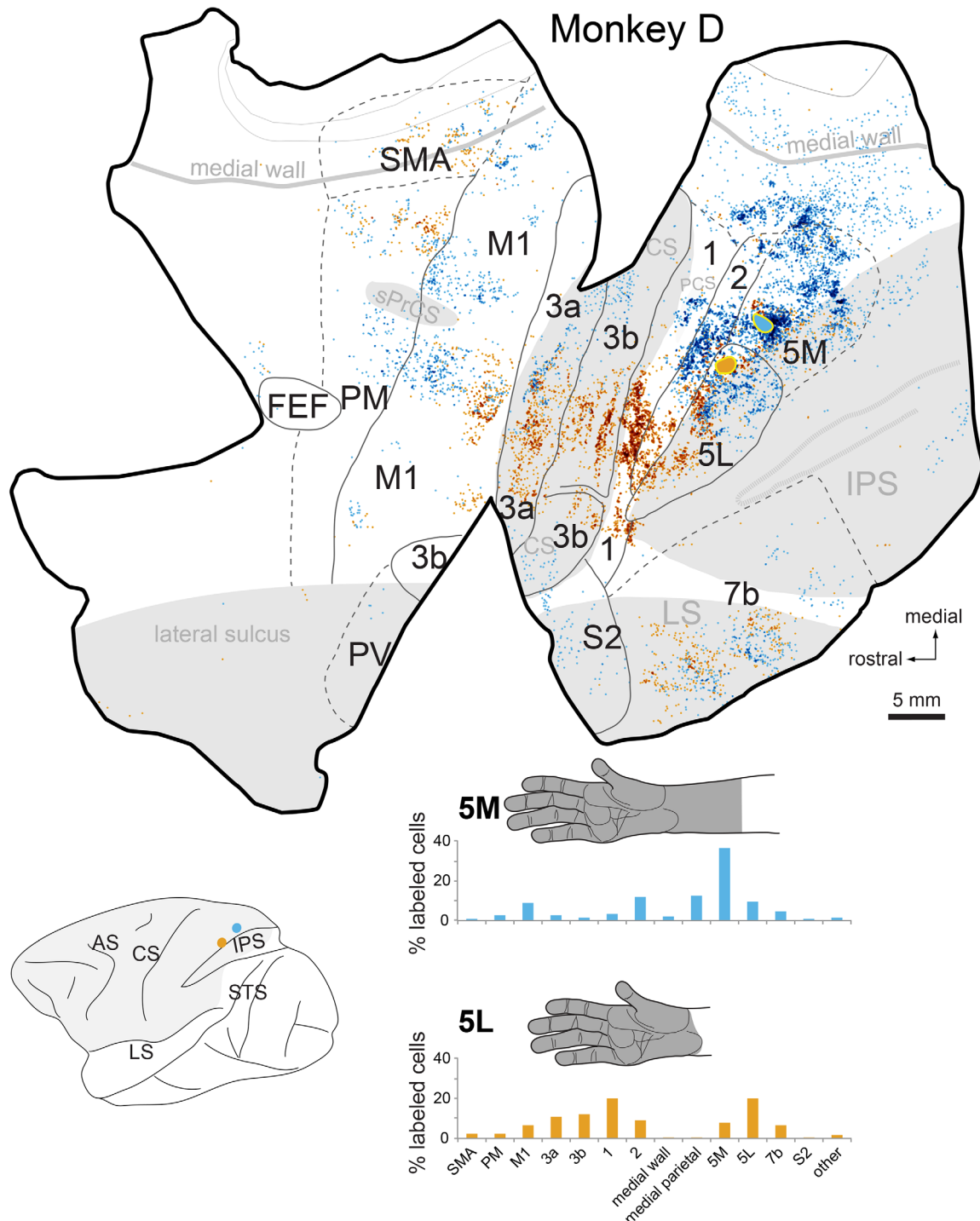
FIGURE 9 An injection of Fluoro-emerald centered in the representation of hand/forearm of area 5M and an injection of Fluoro-ruby centered in the representation of the hand in area 5L. The overall pattern and density of connections in area 5M is similar to that described for the cases in Figures 7 and 8 (also see plots in Figure 6). Connections of area 5L are quite different. First, the density of labeled cells in anterior parietal cortex is much higher than for injections in area 5M. Second, little or no labeling is observed in medial parietal, S2 or cortex on the medial wall. Finally, while connections are observed with M1 and PM, the cells are restricted to a limited portion of these fields, while for injections in 5M, connections are more broadly distributed. Conventions as in previous figures

mediolateral extent of traditionally defined area 5 (see below). Finally, in some earlier studies, when connections were studied via degeneration resulting from lesions in and around area 5/PE, the results were shown only as they related to sulcal patterns, making parcellation of

connections into specific cortical fields hard to evaluate (e.g., Pandya & Seltzer, 1982).

In order to better compare previous studies with our own, we reanalyzed data from some of these previous studies based on the

relative position of the injection site along the rostral bank of the IPS and the PCS (Figure 10); medial versus lateral. We considered the connections of medial and lateral portions of area 5/PE separately and found that the data from injections located medially are consistent with our results on connections of area 5M. Injections in a medial location within area 5 resulted in dense intrinsic connectivity, connections with the S2 region, portions of area 7, and motor cortex (Jones et al., 1978; Pons & Kaas, 1986). Only limited connections were observed with anterior parietal fields. This pattern is consistent with area 5M connections observed in this study. Bakola and colleagues (Bakola et al., 2013) injected neuroanatomical tracers along a large mediolateral extent of area PE, which appears to include portions of functionally and architectonically defined areas 5M, 5L and 2 (compare Figure 1a with Figure 1d; also see (Pons et al., 1985; Seelke et al., 2012). With some exceptions, injections in medial PE (Figure 10b) yielded connection patterns like those of our 5M (Figure 10a). While comparisons of this previous work with the results from the present study are generally in agreement, the reliability of such comparisons is limited by two factors: (1) Different laboratories may use slightly different criteria to determine areal borders. (2) If areal borders were not determined, the accuracy of our estimates of this border based on sulcal patterns are limited by individual variability in the relationship between sulcal patterns and architectonically (Figures 4–5, 7–9) or electrophysiologically (Seelke et al., 2012) defined boundaries.
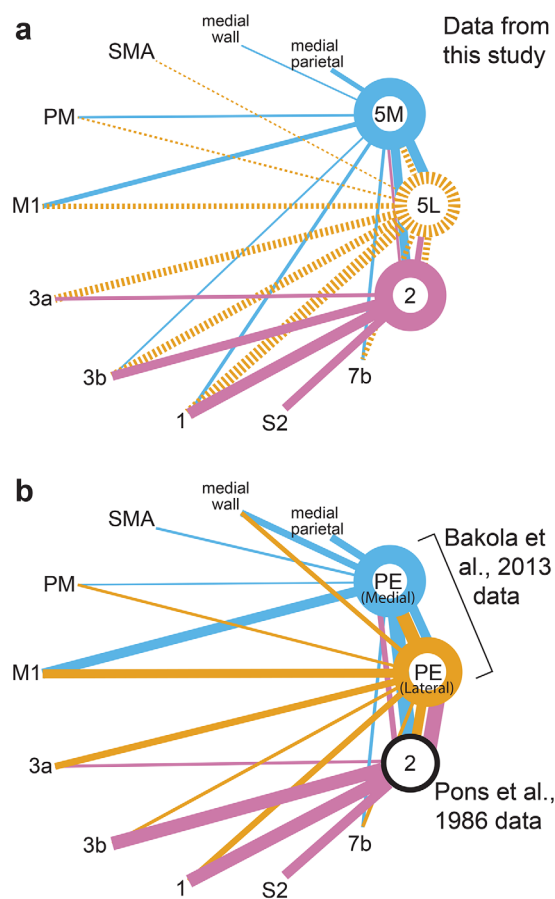
Patterns of connectivity have been described for PPC in New World monkeys and prosimian galagos, but functional data suggest that the status of homology with divisions of area 5 in Old World macaque monkeys is uncertain. As in area 5L, defined with electrophysiological recording techniques, in macaque monkeys (Seelke et al., 2012), area 5 in New World titi monkeys contains only representations of the forelimb, hand and digits, and the map is fractured (Padberg, Disbrow, & Krubitzer, 2005). In cebus monkeys a clear area 2 and area 5 have been identified. Like area 5M in macaque monkeys, area 5 in cebus monkeys is dominated by the representation of the hand and forelimb with only a very small portion devoted to the trunk and hindlimb. In owl monkeys, squirrel monkeys (Gharbawie, Stepniewska, & Kaas, 2011), titi monkeys (Baldwin MKL, 2017) and galagos (Stepniewska, Cerkevich, Fang, & Kaas, 2009), cortex in the region of area 5 has been termed PPC and contains movement domains associated with ethologically relevant behaviors when explored using intracortical microstimulation. Defensive forelimb and face domains have been revealed in the parietal lobe of macaque monkeys, but specifically in VIP (Cooke, Taylor, Moore, & Graziano, 2003); eye movements have been evoked in LIP (Thier & Andersen, 1998); and grasp movements have been evoked in area 2 and area 5 (Gharbawie, Stepniewska, Qi, et al., 2011; Rathelot,

FIGURE 10.

FIGURE 10 Comparison of connectional data in macaques from the present study (a), (Bakola et al., 2013; Pons & Kaas, 1986). (b). Schematic of ipsilateral cortical projections to areas 2, 5M (medial PE) and 5L (lateral PE). Line thickness represents mean normalized connection strengths across cases. To more clearly portray the range of connections strengths we observed, line thickness $\propto$ mean (labeled cells in a field/total labeled cells in hemisphere)$^{0.5}$ minus a constant. Thickness of lines encircling injected fields 5M, 5L, and 2 represents the strength of intrinsic connections—label found outside of the tracer injection halo but within the same cortical field. One exception is the black circle around area 2 in (b), which reflects the fact that intrinsic connection data were not displayed in Pons and Kaas, 1986. Connections that account for less than 2% of labeled cells are not depicted. Data from Table 1 in Bakola and colleagues (Bakola et al., 2013) do not consider label intrinsic to PE, therefore line thicknesses representing connections from both medial and lateral PE in (b) derive from a combination of quantitative data and visual estimates of label density in different parts of PE. We re-interpreted the Bakola et al., study such that 5M is assumed to overlap medial PE, MIP and dMIP; 5L is assumed to overlap lateral PE and PEip. Medial PE injections (e.g., case 1 in (Bakola et al., 2013)) revealed a connection pattern consistent with our injections in area 5M. Lateral PE injections (e.g., case 2 in (Bakola et al., 2013)) revealed connections consistent with an injection mostly in area 5L. Data from Pons and Kaas, (Pons & Kaas, 1986) are counts of the small numbers of labeled cell bodies shown in their Figures 2–4 (cases 83–43, 83–19, and 82–78, respectively), all cases in the macaque forelimb representation with the tracer injection site restricted to area 2. Note that in case 83–19, sections D and E, they depict labeled cells in between tissue identified as area 7 and S2, although no areal border is shown. Given the location of this label in the lateral sulcus, we have included these cells in the counts for S2 connections. Pons and Kaas labeled cells in area 5 are all found laterally (overlapping 5L/lateral PE) except for section A of case 82–78, which are more medial (overlapping 5M/ medial PE)

TABLE 4 Quantification of labeled neurons in cortical fields following area 2 injections by Pons and Kaas, 1986

| Location of cells | Area 2 injections (Pons and Kaas, 1986) | | | | | | Mean | STD |
| | Monkey 83–43 | | Monkey 83–19 | | Monkey 82–78 | | | |
	cells	%	cells	%	cells	%	%	%
4	4	4.44	0	0.00	0	0.00	1.48	2.57
3a	0	0.00	0	0.00	5	6.85	2.28	3.95
3b	26	28.89	13	13.68	21	28.77	23.78	8.74
1	25	27.78	12	12.63	21	28.77	23.06	9.04
2	0	0.00	0	0.00	0	0.00	0.00	0.00
5M	0	0.00	0	0.00	15	20.55	6.85	11.86
5L	31	34.44	33	34.74	11	15.07	28.08	11.27
7	0	0.00	0	0.00	0	0.00	0.00	0.00
S2	4	4.44	37	38.95	0	0.00	14.46	21.32
Total	90	100	95	100.00	73	100		

Dum, & Strick, 2017). Further, in a recent ICMS study in our laboratory, movements of the digits, hand and forelimb could be evoked from areas 2, lateral portions of area 5 and to a more limited extent from 5M in macaque monkeys (Baldwin et al., 2017). Thus, cebus monkeys appear to have an area 5L/5M, and PPC in squirrel monkeys, owl monkeys and galagos may have homologues to areas 5L/5M in Old World monkeys.

The connections of PPC in Old World macaques, New World monkeys, and prosimian primates is variable (Figure 11), and connection patterns depended significantly on the placement of tracer injections within PPC (Burman, Palmer, Gamberini, Spitzer, & Rosa, 2008; Gharbawie, Stepniewska, & Kaas, 2011; Padberg et al., 2005; Stepniewska et al., 2009). Thus, connection patterns do not provide conclusive support for homology of PPC areas across primates. In fact, differences in patterns of connections raise the possibility that different PPC movement domains within New World monkeys and galagos represent different cortical fields.

4.2 | Function/connection relationships in macaque monkeys

While there are differences in the proposed function of portions of architectonically defined area 5, most studies implicate the medial portion of the IPS in translating and combining multiple frames of reference (gaze centered, body centered, head centered) into a common coordinate system or integrated plan for reaching toward a target in immediate extrapersonal space (Buneo et al., 2002). Studies of MIP/area 5M indicate that neurons here may also integrate information about the motor relevance of external sensory cues, and use efference copy to distinguish self-generated movements from externally-caused passive movements to limit reflexive responses to expected sensory inputs resulting from voluntary movements (Kalaska, 1996; Klam & Graf, 2006). Recently, studies demonstrate that in medial area 5 and MIP, multiple frames of reference may actually be mapped onto a

common coordinate system (McGuire & Sabes, 2011), and these maps utilize sensory inputs available to plan movements. The lateral portion of the IPS appears to be involved in the kinematics of reaching, coordinating multiple limb parts for reaching and grasping actions, and matching object properties, such as size and shape, with hand configurations. Area 2 is thought to provide proprioceptive feedback necessary for movement correction (London & Miller, 2013) and is also involved in haptic shape perception (Yau et al., 2013; Yau, Kim, Thakur, & Bensmaia, 2016).

Area 5M is characterized by heavy intrinsic connectivity, perhaps allowing for the selection of a large number of possible movements through activation of a specific combination of internal connections. Strong connections from areas 2 and 5L provide proprioceptive and kinematic information to 5M/MIP, and MIP has been demonstrated to receive additional input about eye position and velocity from the brainstem via the central lateral and ventral lateral nuclei of the thalamus (Prevosto, Graf, & Ugolini, 2009). Additional input about eye position (Wang, Zhang, Cohen, & Goldberg, 2007; Xu, Wang, Peck, & Goldberg, 2011) comes from area 3a. In addition, area 5M/MIP receives motor and premotor inputs (current study; (Matelli, Govoni, Galletti, Kutz, & Luppino, 1998)) which may include efference copy postulated to play a role in MIP functions.

The dominant somatosensory inputs to the lateral portion of PE (5L) would allow this area to integrate information about touch and texture (areas 3b and 1), arm and hand posture (areas 3a and 2), predicted movements and postures (efference copy from M1, PM and SMA) and reach planning activity (5M). Together, this information about current and predicted arm and hand posture (from area 2) could be used by this area in its proposed role in the kinematics of reaching, coordinating multiple limb parts for reaching and grasping actions, and integrating proprioceptive and tactile feedback to adjust or correct hand posture when an object is contacted at the end of a reach (Chen et al., 2009). Finally, projections from areas 3a to area 2 provide information about the current state of muscle contraction, and projections
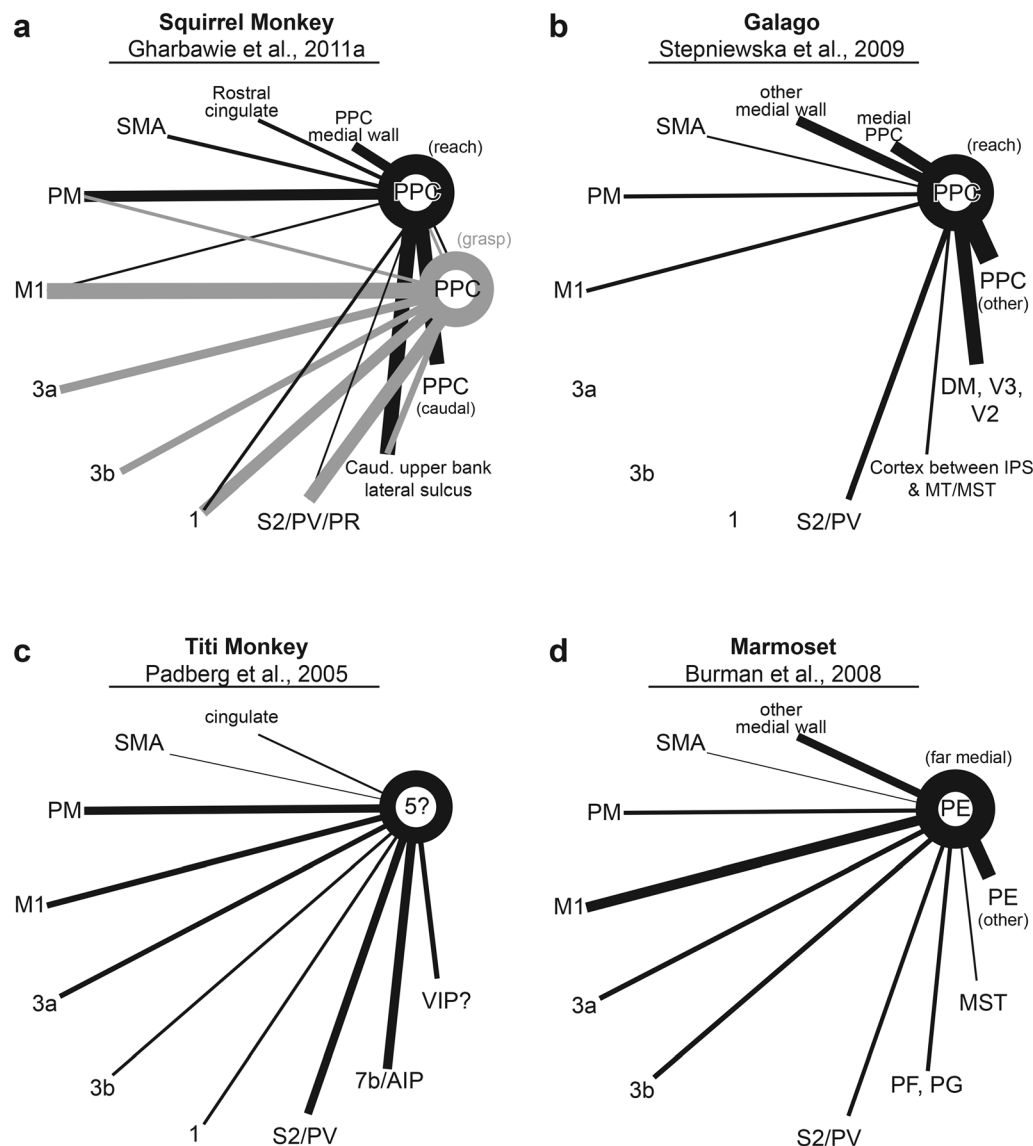
FIGURE 11 Comparison of connectional data in the squirrel monkey (a), prosimian galago (b), titi monkey (c), and marmoset (d). Line thickness represents connection strength. For panel (a), this is derived from quantitative data (see Figure 11 for details; data from Table 2 in (Gharbawie, Stepniewska, & Kaas, 2011)); similar to Figure 11b, representation of intrinsic label is based on visual estimates of label density. For other panels, line thickness is based on visual estimates of label density (b, Figure 7 in (Stepniewska et al., 2009); (c) Figures 10F and 11A in (Padberg et al., 2005); (d) Figure 8B–E in (Burman et al., 2008)). Injection sites in PPC of the squirrel monkey (a) and galago (b) were characterized by movements (reach, grasp) evoked by intracortical microstimulation. Injection sites in presumptive area 5 of the titi monkey (c) were in the somatosensory hand representation. Injections in far medial PE of the marmoset (d) are located adjacent to the midline, perhaps further medial than any homolog to 5M or 5L. Connectional data provide an uncertain picture of PPC homology across New World monkeys, prosimian primates, and Old-World macaques. Some of the patterns of connections are similar to those of macaque areas 5L and 5M. This is especially true for injections that were placed at least a few millimeters from the caudal border of area 1 in New World monkeys (Gharbawie, Stepniewska, & Kaas, 2011), and in the more rostral part of PPC in galagos (Stepniewska et al., 2009)

from areas 3b and 1 provide the tactile information necessary for shape perception. Inputs to area 2 from motor cortex provide information about online volitional movements necessary for distinguishing self-movement from execution errors.

CONFLICT OF INTEREST STATEMENT

The authors have declared that no competing interests exist.

ROLE OF AUTHORS

ORCID

Jeffrey Padberg http://orcid.org/0000-0002-0522-0120

Jon H. Kaas http://orcid.org/0000-0002-9985-1192

REFERENCES

Almecija, S., & Sherwood, C. C. (2017). Hands, brains and precision grips: Origins of tool use behaviors. In K. J. Krubitzer (Ed.), *Primates* (2nd ed., Vol. *3*, pp. 299–315). London: Elsevier.

Bakola, S., Passarelli, L., Gamberini, M., Fattori, P., & Galletti, C. (2013). Cortical connectivity suggests a role in limb coordination for macaque area PE of the superior parietal cortex. *J Neurosci*, *33*(15), 6648–6658. https://doi.org/10.1523/JNEUROSCI.4685-12.2013

Baldwin, M. K. L., Cooke, D. F., Goldring, A. B., & Krubitzer, L. (2017). Representations of fine digit movements in posterior and anterior parietal cortex revealed using long-train intracortical microstimulation in macaque monkeys. *Cerebral Cortex*, 1–20. https://doi.org/10.1093/cercor/bhx279

Baldwin, M. K. L., H, A., & Krubitzer, L. A. (2017). *The functional organization of movement maps in New World Titi monkeys*. Society for Neuroscience Abstracts 316.06.

Brodmann, K. (1909). *Localisation in the cerebral cortex* Leipzig: Bart-Verlag.

Bruce, K., & Grofova, I. (1992). Notes on a light and electron microscopic double-labeling method combining anterograde tracing with Phaseolus vulgaris leucoagglutinin and retrograde tracing with cholera toxin subunit B. *Journal of Neuroscience Methods*, *45*(1–2), 23–33.

Buneo, C. A., Jarvis, M. R., Batista, A. P., & Andersen, R. A. (2002). Direct visuomotor transformations for reaching. *Nature*, *416*, 632–636.

Burman, K. J., Palmer, S. M., Gamberini, M., Spitzer, M. W., & Rosa, M. G. (2008). Anatomical and physiological definition of the motor cortex of the marmoset monkey. *The Journal of Comparative Neurology*, *506*(5), 860–876. https://doi.org/10.1002/cne.21580

Chaplin, T. A., Rosa, M., & Yu, H.-H. (2017). Scaling up the simian primate cortex: A conserved pattern of expansion across brain sizes. In L. a. K. J. Krubitzer (Ed.), *Primates* (2nd ed., Vol. *3*, pp. 99–111). London: Elsevier.

Chen, J., Reitzen, S. D., Kohlenstein, J. B., & Gardner, E. P. (2009). Neural representation of hand kinematics during prehension in posterior parietal cortex of the macaque monkey. *Journal of Neurophysiology*, *102*(6), 3310–3328. https://doi.org/10.1152/jn.90942.2008

Colby, C. L., & Duhamel, J. R. (1991). Heterogeneity of extrastriate visual areas and multiple parietal areas in the macaque monkey. *Neuropsychologia*, *29*(6), 517–537.

Colby, C. L., & Duhamel, J. R. (1996). Spatial representations for action in parietal cortex. *Brain Research Cognitive Brain Research*, *5*(1–2), 105–115.

Cooke, D. F., Padberg, J., Zahner, T., & Krubitzer, L. (2012). The functional organization and cortical connections of motor cortex in squirrels. *Cerebral Cortex*, *22*(9), 1959–1978. https://doi.org/10.1093/cercor/bhr228

Cooke, D. F., Taylor, C. S., Moore, T., & Graziano, M. S. (2003). Complex movements evoked by microstimulation of the ventral intraparietal area. *Proceedings of the National Academy of Sciences of the United States of America*, *100*(10), 6163–6168. https://doi.org/10.1073/pnas.1031751100 1031751100 [pii]

Delhaye, B. P., L, K., & Bensmaia, S. J. (2017). *Neural Basis of touch and proprioception in the cortex of primates*. Comprehensive Physiology.

Disbrow, E., Litinas, E., Recanzone, G., Padberg, J. P., & Krubitzer, L. A. (2003). Cortical connections of the parietal central area and the second somatosensory area in macaque monkeys. *The Journal of Comparative Neurology*, *462*, 382–399.

Gallyas, F. (1979). Silver staining of myelin by means of physical development. *Neurological Research*, *1*, 203–209.

Gardner, E. P., Babu, K. S., Ghosh, S., Sherwood, A., & Chen, J. (2007). Neurophysiology of prehension. III. Representation of object features in posterior parietal cortex of the macaque monkey. *Journal of Neurophysiology*, *98*(6), 3708–3730. https://doi.org/10.1152/jn.00609.2007

Gardner, E. P., Babu, K. S., Reitzen, S. D., Ghosh, S., Brown, A. S., Chen, J., ... Ro, J. Y. (2007). Neurophysiology of prehension. I. Posterior parietal cortex and object-oriented hand behaviors. *Journal of Neurophysiology*, *97*(1), 387–406. https://doi.org/10.1152/jn.00558.2006

Gharbawie, O. A., Stepniewska, I., & Kaas, J. H. (2011). Cortical connections of functional zones in posterior parietal cortex and frontal cortex motor regions in new world monkeys. *Cerebral Cortex*, *21*(9), 1981–2002. https://doi.org/10.1093/cercor/bhq260

Gharbawie, O. A., Stepniewska, I., Qi, H., & Kaas, J. H. (2011). Multiple parietal-frontal pathways mediate grasping in macaque monkeys. *Journal of Neuroscience*, *31*(32), 11660–11677. https://doi.org/10.1523/JNEUROSCI.1777-11.2011

Glasser, M. F., Coalson, T. S., Robinson, E. C., Hacker, C. D., Harwell, J., Yacoub, E., ... Van Essen, D. C. (2016). A multi-modal parcellation of human cerebral cortex. *Nature*, *536*(7615), 171–178. https://doi.org/10.1038/nature18933

Glasser, M. F., Goyal, M. S., Preuss, T. M., Raichle, M. E., & Van Essen, D. C. (2014). Trends and properties of human cerebral cortex: correlations with cortical myelin content. *Neuroimage*, *93 Pt 2*, 165–175. https://doi.org/10.1016/j.neuroimage.2013.03.060

Godschalk, M., Mitz, A. R., van Duin, B., & van der Burg, H. (1995). Somatotopy of monkey premotor cortex examined with microstimulation. *Neuroscience Research*, *23*(3), 269–279.

Goldring, A. B., & Krubitzer, L. (2017). Evolution of the parietal cortex in mammals: From manipulation to tool use. In L. Krubitzer, & J. H. Kaas (Ed.), *The Evolution of Nervous Systems* (2nd ed., Vol. *3*, pp. 259–286). London: Elsevier.

Gould, H. J. I., Cusick, C. G., Pons, T. P., & Kaas, J. H. (1986). The relationship of corpus callosum connections to electrical stimulation maps of motor, supplementary motor, and the frontal eye fields in owl monkeys. *The Journal of Comparative Neurology*, *247*, 297–325.

Gregoriou, G. G., Borra, E., Matelli, M., & Luppino, G. (2006). Architectonic organization of the inferior parietal convexity of the macaque monkey. *The Journal of Comparative Neurology*, *496*, 422–451.

Hyvarinen, J., & Poranen, A. (1978a). Movement-sensitive and direction and orientation-selective cutaneous receptive fields in the hand area of the post-central gyrus in monkeys. *The Journal of Physiology*, *283*, 523–537.

Hyvarinen, J., & Poranen, A. (1978b). Receptive field integration and sub-modality convergence in the hand area of the post-central gyrus of the alert monkey. *The Journal of Physiology*, *283*, 539–556.

Iwamura, Y., Tanaka, M., Sakamoto, M., & Hikosaka, O. (1993). Rostro-caudal gradients in the neuronal receptive field complexity in the finger region of the alert monkey's postcentral gyrus. *Experimental Brain Research*, *92*(3), 360–368.

Jones, E. G., Coulter, J. D., & Hendry, S. H. (1978). Intracortical connectivity of architectonic fields in the somatic sensory, motor and parietal cortex of monkeys. *The Journal of Comparative Neurology*, *181*(2), 291–347. https://doi.org/10.1002/cne.901810206

Kaas, J. H., & Stepniewska, I. (2016). Evolution of posterior parietal cortex and parietal-frontal networks for specific actions in primates. *Journal of Comparative Neurology*, *524*(3), 595–608. https://doi.org/10.1002/cne.23838

Kalaska, J. F. (1996). Parietal cortex area 5 and visuomotor behavior. *Canadian Journal of Physiology and Pharmacology*, *74*, 483–498.

Klam, F., & Graf, W. (2006). Discrimination between active and passive head movements by macaque ventral and medial intraparietal cortex neurons. *The Journal of Physiology*, *574*(Pt 2), 367–386. https://doi.org/10.1113/jphysiol.2005.103697

Krubitzer, L., Clarey, J., Tweedale, R., Elston, G., & Calford, M. (1995). A redefinition of somatosensory areas in the lateral sulcus of macaque monkeys. *The Journal of Neuroscience*, *15*(5 Pt 2), 3821–3839.

Krubitzer, L., Huffman, K. J., Disbrow, E., & Recanzone, G. (2004). Organization of area 3a in macaque monkeys: Contributions to the cortical phenotype. *The Journal of Comparative Neurology*, *471*(1), 97–111.

Lewis, J., & Van Essen, D. (2000). Mapping of architectonic subdivisions in the macaque monkey, with emphasis on parieto-occipital cortex. *The Journal of Comparative Neurology*, *428*, 79–111.

London, B. M., & Miller, L. E. (2013). Responses of somatosensory area 2 neurons to actively and passively generated limb movements. *Journal of Neurophysiology*, *109*(6), 1505–1513. https://doi.org/10.1152/jn.00372.2012

Matelli, M., Luppino, G., & Rizzolati, G. (1985). Patterns of cytochrome oxidase activity in the frontal agranular cortex of the macaque monkey. *Behaviour Brain Research*, *18*, 125–136.

Matelli, M., Govoni, P., Galletti, C., Kutz, D. F., & Luppino, G. (1998). Superior area 6 afferents from the superior parietal lobule in the macaque monkey. *The Journal of Comparative Neurology*, *402*(3), 327–352.

McGuire, L. M., & Sabes, P. N. (2009). Sensory transformations and the use of multiple reference frames for reach planning. *Nature Neuroscience*, *12*(8), 1056–1061. https://doi.org/10.1038/nn.2357

McGuire, L. M., & Sabes, P. N. (2011). Heterogeneous representations in the superior parietal lobule are common across reaches to visual and proprioceptive targets. *Journal of Neuroscience*, *31*(18), 6661–6673. https://doi.org/10.1523/JNEUROSCI.2921-10.2011

Mountcastle, V. B., Lynch, J. C., Georgopoulos, A., Sakata, H., & Acuna, C. (1975). Posterior parietal association cortex of the monkey: command functions for operations within extrapersonal space. *Journal of Neurophysiology*, *38*(4), 871–908.

Nelissen, K., & Vanduffel, W. (2011). Grasping-related functional magnetic resonance imaging brain responses in the macaque monkey. *The Journal of Neuroscience*, *31*(22), 8220–8229. https://doi.org/10.1523/JNEUROSCI.0623-11.2011

Nelson, R. J., Sur, M., Felleman, D. J., & Kaas, J. H. (1980). Representations of the body surface in postcentral parietal cortex of *Macaca fascicularis*. *The Journal of Comparative Neurology*, *192*(4), 611–643. https://doi.org/10.1002/cne.901920402

Padberg, J., Disbrow, E., & Krubitzer, L. (2005). The organization and connections of anterior and posterior parietal cortex in titi monkeys: Do New World monkeys have an area 2?. *Cerebral Cortex*, *15*(12), 1938–1963. https://doi.org/10.1093/cercor/bhi071

Padberg, J., Recanzone, G., Engle, J., Cooke, D., Goldring, A., & Krubitzer, L. (2010). Lesions in posterior parietal area 5 in monkeys result in rapid behavioral and cortical plasticity. *Journal of Neuroscience*, *30*(39), 12918–12935. https://doi.org/10.1523/JNEUROSCI.1806-10.2010

Pandya, D. N., & Seltzer, B. (1982). Intrinsic connections and architectonics of posterior parietal cortex in the rhesus monkey. *The Journal of Comparative Neurology*, *204*, 196–210.

Pons, T. P., Garraghty, P. E., Cusick, C. G., & Kaas, J. H. (1985). The somatotopic organization of area 2 in macaque monkeys. *The Journal of Comparative Neurology*, *241*(4), 445–466. https://doi.org/10.1002/cne.902410405

Pons, T. P., & Kaas, J. H. (1986). Corticocortical connections of area 2 of somatosensory cortex in macaque monkeys: a correlative anatomical and electrophysiological study. *The Journal of Comparative Neurology*, *248*(3), 313–335. https://doi.org/10.1002/cne.902480303

Preuss, T. M., Stepniewska, I., & Kaas, J. H. (1996). Movement representation in the dorsal and ventral premotor areas of owl monkeys: A microstimulation study. *The Journal of Comparative Neurology*, *371*, 649–676.

Prevosto, V., Graf, W., & Ugolini, G. (2009). Posterior parietal cortex areas MIP and LIPv receive eye position and velocity inputs via ascending preposito-thalamo-cortical pathways. *European Journal of Neuroscience*, *30*(6), 1151–1161. https://doi.org/10.1111/j.1460-9568.2009.06885.x

Rathelot, J. A., Dum, R. P., & Strick, P. L. (2017). Posterior parietal cortex contains a command apparatus for hand movements. *Proceedings of the National Academy of Sciences of the United States of America*, *114*(16), 4255–4260. https://doi.org/10.1073/pnas.1608132114

Rothemund, Y., Qi, H. X., Collins, C. E., & Kaas, J. H. (2002). The genitals and gluteal skin are represented lateral to the foot in anterior parietal somatosensory cortex of macaques. *Somatosensory and Motor Research*, *19*(4), 302–315. https://doi.org/10.1080/0899022021000037773

Rozzi, S., Calzavara, R., Belmalih, A., Borra, E., Gregoriou, G. G., Matelli, M., & Luppino, G. (2006). Cortical connections of the inferior parietal cortical convexity of the macaque monkey. *Cerebral Cortex*, *16*, 1389–1417.

Rozzi, S., Ferrari, P. F., Bonini, L., Rizzolatti, G., & Fogassi, L. (2008). Functional organization of inferior parietal lobule convexity in the macaque monkey: Electrophysiological characterization of motor, sensory and mirror responses and their correlation with cytoarchitectonic areas. *European Journal of Neuroscience*, *28*(8), 1569–1588. https://doi.org/10.1111/j.1460-9568.2008.06395.x

Scherberger, H., Fineman, I., Musallam, S., Dubowitz, D. J., Bernheim, K. A., Pesaran, B., … Andersen, R. A. (2003). Magnetic resonance image-guided implantation of chronic recording electrodes in the macaque intraparietal sulcus. *Journal of Neuroscience Methods*, *130*(1), 1–8.

Schieber, M. H. (2001). Constraints on somatotopic organization in the primary motor cortex. *Journal of Neurophysiology*, *86*(5), 2125–2143.

Seelke, A. M., Padberg, J. J., Disbrow, E., Purnell, S. M., Recanzone, G., & Krubitzer, L. (2012). Topographic maps within brodmann's area 5 of macaque monkeys. *Cerebral Cortex*, *22*(8), 1834–1850. https://doi.org/10.1093/cercor/bhr257

Seltzer, B., & Pandya, D. N. (1986). Posterior parietal projections to the intraparietal sulcus of the rhesus monkey. *Experimental Brain Research*, *62*(3), 459–469.

Sincich, L. C., Jocson, C. M., & Horton, J. C. (2010). V1 interpatch projections to v2 thick stripes and pale stripes. *Journal of Neuroscience, 30*(20), 6963–6974. https://doi.org/10.1523/JNEUROSCI.5506-09.2010

Snyder, L. H., Batista, A. P., & Andersen, R. A. (1997). Coding of intention in the posterior parietal cortex. *Nature, 386*(6621), 167–170. https://doi.org/10.1038/386167a0

Snyder, L. H., Batista, A. P., & Andersen, R. A. (1998). Change in motor plan, without a change in the spatial locus of attention, modulates activity in posterior parietal cortex. *Journal of Neurophysiology, 79*(5), 2814–2819.

Stepniewska, I., Cerkevich, C. M., Fang, P. C., & Kaas, J. H. (2009). Organization of the posterior parietal cortex in galagos: II. Ipsilateral cortical connections of physiologically identified zones within anterior sensorimotor region. *The Journal of Comparative Neurology, 517*(6), 783–807. https://doi.org/10.1002/cne.22190

Stepniewska, I., Fang, P. C., & Kaas, J. H. (2005). Microstimulation reveals specialized subregions for different complex movements in posterior parietal cortex of prosimian galagos. *Proceedings of the National Academy of Sciences the United States of America, 102*(13), 4878–4883. https://doi.org/0501048102 [pii] 10.1073/pnas.0501048102

Thier, P., & Andersen, R. A. (1998). Electrical microstimulation distinguishes distinct saccade-related areas in the posterior parietal cortex. *Journal of Neurophysiology, 80*(4), 1713–1735.

Wang, X., Zhang, M., Cohen, I. S., & Goldberg, M. E. (2007). The proprioceptive representation of eye position in monkey primary somatosensory cortex. *Nature Neuroscience, 10*(5), 640–646. https://doi.org/10.1038/nn1878

Wong-Riley, M. (1979). Changes in the visual system of monocularly sutured or enucleated cats demonstrable with cytochrome oxidase histochemistry. *Brain Research, 171*, 11–28.

Xu, Y., Wang, X., Peck, C., & Goldberg, M. E. (2011). The time course of the tonic oculomotor proprioceptive signal in area 3a of somatosensory cortex. *Journal of Neurophysiology, 106*(1), 71–77. https://doi.org/10.1152/jn.00668.2010

Yau, J. M., Connor, C. E., & Hsiao, S. S. (2013). Representation of tactile curvature in macaque somatosensory area 2. *Journal of Neurophysiology, 109*(12), 2999–3012. https://doi.org/10.1152/jn.00804.2012

Yau, J. M., Kim, S. S., Thakur, P. H., & Bensmaia, S. J. (2016). Feeling form: The neural basis of haptic shape perception. *Journal of Neurophysiology, 115*(2), 631–642. https://doi.org/10.1152/jn.00598.2015